



Short communication

## Formation of the high lithium ion conducting phase from mechanically milled amorphous $\text{Li}_2\text{S}-\text{P}_2\text{S}_5$ system

Junghoon Kim<sup>a</sup>, Yongsu Yoon<sup>a</sup>, Jiho Lee<sup>b</sup>, Dongwook Shin<sup>a,\*</sup><sup>a</sup> Division of Materials Science & Engineering, Hanyang University, 17 Haengdang-dong, Seongdong-gu, Seoul 133-791, Republic of Korea<sup>b</sup> Department of Fuel Cells and Hydrogen Technology, Hanyang University, 17 Haengdang-dong, Seongdong-gu, Seoul 133-791, Republic of Korea

## ARTICLE INFO

## Article history:

Received 13 September 2010

Received in revised form

30 November 2010

Accepted 8 December 2010

Available online 21 December 2010

## Keywords:

Lithium ion battery

Solid electrolyte

Lithium phosphorous sulfide

Mechanical milling

## ABSTRACT

The fast ionic conducting structure similar to thio-Lithium Super Ionic Conductor (LISICON) phase is synthesized in the  $\text{Li}_2\text{S}-\text{P}_2\text{S}_5$  system. The  $\text{Li}_2\text{S}-\text{P}_2\text{S}_5$  glass-ceramics with the composition of  $x\text{Li}_2\text{S} \cdot (100-x)\text{P}_2\text{S}_5$  ( $75 \leq x \leq 80$ ) are prepared by the heat-treatment of mechanically milled amorphous sulfide powders. In the binary  $\text{Li}_2\text{S}-\text{P}_2\text{S}_5$  system,  $78.3\text{Li}_2\text{S} \cdot 21.7\text{P}_2\text{S}_5$  glass ceramic prepared by mechanical milling and subsequent heat-treatment at  $260^\circ\text{C}$  for 3 h shows the highest conductivity of  $6.3 \times 10^{-4} \text{ S cm}^{-1}$  at room temperature and the lowest activation energy for conduction of  $30.5 \text{ kJ mol}^{-1}$ . The enhancement of conductivity with increasing  $x$  up to 78.3 is probably caused by the introduction of interstitial lithium ions at the Li sites which affects the Li ion distribution. The prepared electrolyte exhibits the lithium ion transport number of almost unity and voltage stability of 5 V vs. Li at room temperature.

© 2010 Elsevier B.V. All rights reserved.

### 1. Introduction

All-solid-state lithium ion batteries based on solid electrolytes have attracted attention in recent years due to increased concerns on the safety problems of commercial lithium ion batteries employing liquid electrolyte [1–3]. Despite its performance, the liquid electrolytes have many disadvantages, such as solvent leakage, flammability and narrow range of operating temperature. Therefore, as a possible solution to this safety issues, it becomes an impending task to develop solid electrolytes with high lithium ion conductivity comparable to that of liquid electrolytes.

For inorganic electrolytes, most of the oxide based electrolytes have low Li ion conductivities below  $10^{-5} \text{ S cm}^{-1}$  at room temperature except for some crystalline materials such as perovskite ( $\text{ABO}_3$ )-type lithium lanthanum titanate (LLTO) and NASICON-type  $\text{Li}_{1.3}\text{Al}_{0.3}\text{Ti}_{1.7}(\text{PO}_4)_3$  (LATP) [4]. However, the low conductivities can be improved by the replacing anion backbone from oxygen to sulfur having the larger ionic size and higher dielectric polarizability. The sulfide-based electrolytes generally have higher lithium ion conductivity by several orders of magnitude than oxide-based electrolytes. For example, the oxide LISICON shows the conductivities of  $\sim 10^{-7} \text{ S cm}^{-1}$  for  $\text{Li}_{14}\text{Zn}(\text{GeO}_4)_4$  [5], while a series of sulfide crystalline lithium fast ionic conductors, thio-LISICON, such as solid solutions in the systems  $\text{Li}_4\text{SiS}_4-\text{Li}_3\text{PS}_4$  and  $\text{Li}_4\text{GeS}_4-\text{Li}_3\text{PS}_4$ , have

been reported to show the maximum conductivities of  $6.4 \times 10^{-4}$  and  $2.2 \times 10^{-3} \text{ S cm}^{-1}$ , respectively [6,7].

It has been reported that the new thio-LISICON was found in the  $\text{Li}_2\text{S}-\text{P}_2\text{S}_5$  binary system prepared by solid state reaction [8]. The obtained material showed high ionic conductivity of  $1.5 \times 10^{-4} \text{ S cm}^{-1}$  at room temperature and high electrochemical stability which is attributed to the absence of strong network formers such as germanium and silicon. Recently, the glass-ceramics prepared from the mechanically milled  $50(0.67\text{Li}_2\text{S} \cdot 0.33\text{SiS}_2) \cdot 50(0.75\text{Li}_2\text{S} \cdot 0.25\text{P}_2\text{S}_5)$  glass, which corresponds to the composition of  $\text{Li}_{3.4}\text{Si}_{0.4}\text{P}_{0.6}\text{S}_4$ , exhibited the highest conductivity of  $1.2 \times 10^{-3} \text{ S cm}^{-1}$ , which is higher than the maximum conductivity  $6.4 \times 10^{-4} \text{ S cm}^{-1}$  of the solid solutions in the system  $\text{Li}_4\text{SiS}_4-\text{Li}_3\text{PS}_4$  prepared by solid state reaction [9]. This work demonstrated that the mechanical milling is a simple and easy method to produce thio-LISICON electrolyte composed of unconventional crystalline phases with high ionic mobility. For bulk electrolytes prepared by the processes such as solid state reaction and melting-quenching, an additional polishing or pulverization is needed to apply to electrolytes in the solid-state batteries, while the mechanically milled electrolyte powders can be directly used as prepared form [10,11].

The mechanical milling was applied to simple  $\text{Li}_2\text{S}-\text{P}_2\text{S}_5$  system and it has been reported that the thio-LISICON II analogue was precipitated in the Li-rich  $80\text{Li}_2\text{S} \cdot 20\text{P}_2\text{S}_5$  glass by heat-treatment at first crystallization temperature while the thio-LISICON III analogue was precipitated in the  $75\text{Li}_2\text{S} \cdot 25\text{P}_2\text{S}_5$  glass [12–14]. The  $80\text{Li}_2\text{S} \cdot 20\text{P}_2\text{S}_5$  glass-ceramic with thio-LISICON II analogue

\* Corresponding author. Tel.: +82 2 2220 0503; fax: +82 2 2220 4011.  
E-mail address: [dwshin@hanyang.ac.kr](mailto:dwshin@hanyang.ac.kr) (D. Shin).

exhibited a room temperature conductivity of  $7.2 \times 10^{-4} \text{ S cm}^{-1}$ , which is 2.6 times larger than the value of  $2.8 \times 10^{-4} \text{ S cm}^{-1}$  for the  $75\text{Li}_2\text{S}\cdot 25\text{P}_2\text{S}_5$  glass–ceramic. However, the composition range studied in the literature was limited to only two compositions. It is not easy to judge the general trend in compositional variation of precipitated thio-LISICON phases and ionic conductivities of the precipitated phases from only two compositions. Also it is needed to verify the possibility to form the thio-LISICON III analogue with comparable or higher conductivity than the thio-LISICON II analogue.

Therefore, the thio-LISICON structure was synthesized from the mechanically milled amorphous  $\text{Li}_2\text{S}\text{--}\text{P}_2\text{S}_5$  system in the subdivided composition range, and its conductivities and basic electrochemical properties were identified. The obtained thio-LISICON phase was compared with the counterpart produced by solid state reaction.

## 2. Experimental

The  $x\text{Li}_2\text{S}\cdot(100-x)\text{P}_2\text{S}_5$  glass–ceramics ( $75 \leq x \leq 80$ ) were prepared by mechanical milling and the subsequent heat-treatment. Reagent-grade  $\text{Li}_2\text{S}$  (Alfa, 99.9%) and  $\text{P}_2\text{S}_5$  (Aldrich, 99%) powders were used as starting materials for mechanical ball milling. These were weighed, mixed in appropriate molar ratios in an argon-filled glove box and put into an alumina pot (volume of 75 mL) with ten alumina balls (10 mm in diameter). Mechanical milling was performed for 20 h using a high energy planetary ball mill apparatus (Fritsch Pulverisette 5). In order to maintain room temperature, milling was conducted by milling for 30 min and resting for 30 min repeatedly. The rotation speed was fixed at 300 rpm.

X-ray diffraction (XRD) measurements were carried out using an X-ray diffractometer (Rigaku Ultima IV) with  $\text{Cu K}\alpha$  radiation. To avoid the attack of water and oxygen in air, samples were sealed in an airtight container covered with polyimide thin film and mounted on the X-ray diffractometer. The diffraction data were collected at each  $0.014^\circ$  step width over a  $2\theta$  range from  $10^\circ$  to  $70^\circ$ .

Ionic conductivities were measured for the pelletized samples. The mechanically milled samples were pelletized by the cold uniaxial press under 4 metric tons and heated up to various temperatures over crystallization temperatures. The diameter and thickness of the pellets were 16 mm and about 1 mm, respectively. Carbon paste was painted as the electrodes on both faces of the pelletized sample and dried at  $120^\circ\text{C}$  for 5 h. AC impedance measurements were carried out in dry Ar atmosphere using a Solartron 1260 impedance analyzer in the frequency range of 10 Hz–5 MHz. DC polarization was also measured to determine a lithium ion transport number of the samples. Lithium plates and SUS plates were attached onto both faces of the pelletized sample as non-blocking electrodes and blocking electrodes, respectively.

The electrochemical stability of the asymmetric  $\text{Li}/78.3\text{Li}_2\text{S}\cdot 21.7\text{P}_2\text{S}_5$  glass–ceramic/SUS cell was evaluated by using cyclic voltammetry. The cyclic voltammogram was obtained using a Solartron 1287 electrochemical interface at the scan rate of  $5 \text{ mV s}^{-1}$  in the scan range between  $-0.3$  and  $5 \text{ V}$ .

## 3. Results and discussion

Fig. 1 shows the XRD patterns of the  $x\text{Li}_2\text{S}\cdot(100-x)\text{P}_2\text{S}_5$  ( $75 \leq x \leq 80$ ) samples mechanically milled for 20 h. Only halo patterns without distinct peaks were observed for  $x \leq 78.3$ , indicating that these samples became amorphous by mechanical milling for 20 h. However, the XRD peaks due to  $\text{Li}_2\text{S}$  crystal appeared along with halo patterns in the samples with  $x \geq 79.1$ . The peak intensities of  $\text{Li}_2\text{S}$  crystal increased with increasing  $x$ . Even after

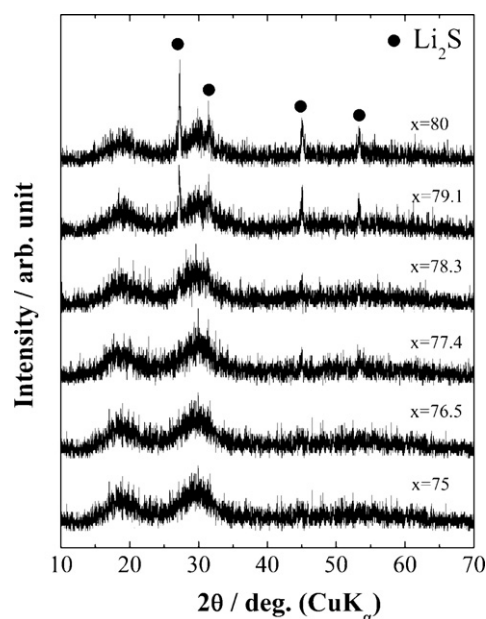


Fig. 1. XRD patterns of the  $x\text{Li}_2\text{S}\cdot(100-x)\text{P}_2\text{S}_5$  ( $75 \leq x \leq 80$ ) samples mechanically milled for 20 h.

mechanical milling for 40 h, the samples with  $x \geq 79.1$  could not be fully amorphized and the glass forming region of the samples was limited to the composition of  $x \leq 78.3$ . Zang and Kennedy have reported that the glass forming region of the  $\text{Li}_2\text{S}\text{--}\text{P}_2\text{S}_5$  glass for melting-quenching process was limited to the compositions of  $x \leq 70$  in the  $x\text{Li}_2\text{S}\cdot(100-x)\text{P}_2\text{S}_5$  [15]. Therefore it is clear that the mechanical milling is more effective to extend the glass forming region.

Fig. 2 shows the XRD patterns of the  $x\text{Li}_2\text{S}\cdot(100-x)\text{P}_2\text{S}_5$  glass–ceramics ( $75 \leq x \leq 80$ ) prepared by heat-treatment of mechanically milled powders at  $260^\circ\text{C}$  for 3 h. Crystalline phases

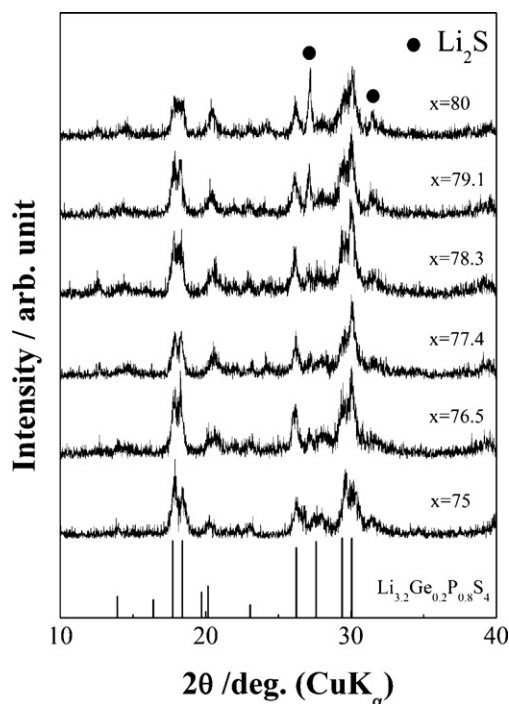
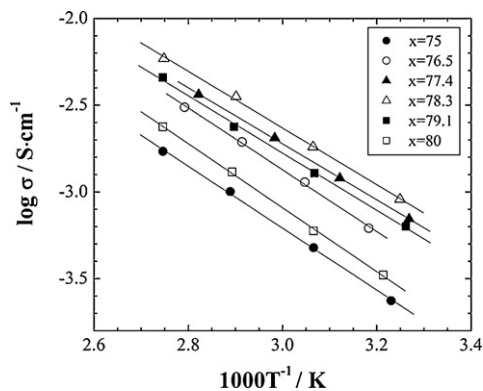


Fig. 2. XRD patterns of the  $x\text{Li}_2\text{S}\cdot(100-x)\text{P}_2\text{S}_5$  glass–ceramics ( $75 \leq x \leq 80$ ) prepared by heat-treatment of mechanically milled powders at  $260^\circ\text{C}$  for 3 h.



**Fig. 3.** Temperature dependence of the conductivities for the  $x\text{Li}_2\text{S}-(100-x)\text{P}_2\text{S}_5$  glass-ceramics ( $75 \leq x \leq 80$ ) prepared by heat-treatment of mechanically milled powders at  $260^\circ\text{C}$  for 3 h.

similar to the thio-LISICON III crystals ( $\text{Li}_{3.2}\text{Ge}_{0.2}\text{P}_{0.8}\text{S}_4$ ) were formed over the whole composition range of  $x = 75$  to  $x = 80$ . However, one can see that the  $\text{Li}_2\text{S}$  crystal peaks remained even after heat-treatment.

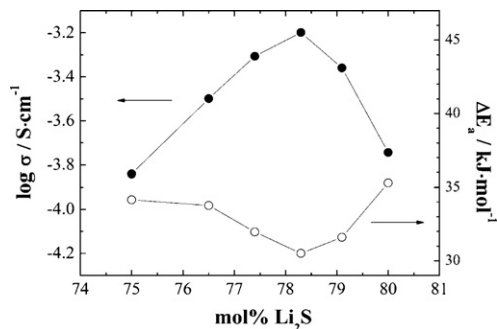
It has been reported that the phases of thio-LISICON  $\text{Li}_{4-x}\text{Ge}_{1-x}\text{P}_x\text{S}_4$  are divided into three composition ranges: range I ( $0 < x \leq 0.6$ ), range II ( $0.6 < x < 0.8$ ) and range III ( $0.8 \leq x < 1.0$ ) [7]. In particular, the thio-LISICON II and III phases in the  $\text{Li}_{4-x}\text{Ge}_{1-x}\text{P}_x\text{S}_4$  solid solution show high room-temperature-conductivities ( $>10^{-4} \text{ S cm}^{-1}$ ). It is noteworthy that the XRD patterns obtained in this work are similar to that of thio-LISICON III in the  $\text{Li}_4\text{GeS}_4\text{-Li}_3\text{PS}_4$  system although two material systems have different compositions.

Previous literatures [12–14] reported, however, that thio-LISICON II phase was precipitated in the composition of  $x = 80$  while Thio-LISICON III phase was precipitated in this work. This is probably due to the different heat-treatment conditions and the temperature dependent stability of phases. Thio-LISICON II and III analogues which were not obtained by solid-state reaction have been reported as thermodynamically unstable phases. Also, thio-LISICON III analogues are more stable than thio-LISICON II analogues at higher temperature. Therefore, the heat-treatment at slightly higher temperature probably resulted in the formation of more stable thio-LISICON III phases.

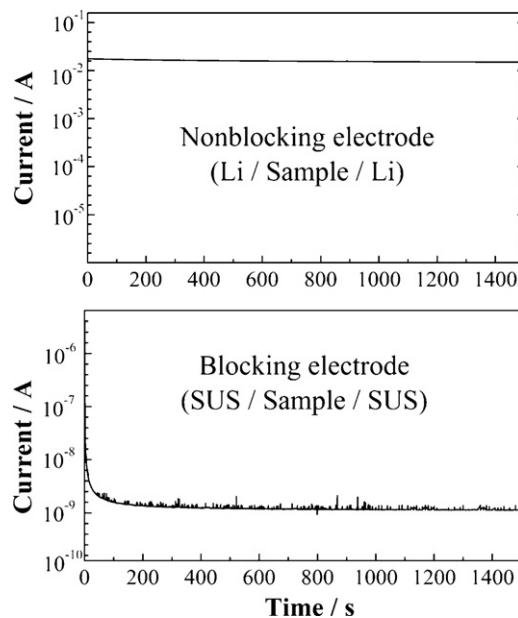
The temperature dependence of the conductivities for  $x\text{Li}_2\text{S}-(100-x)\text{P}_2\text{S}_5$  glass-ceramics ( $75 \leq x \leq 80$ ) prepared by heat-treatment of mechanically milled powders at  $260^\circ\text{C}$  for 3 h are shown in Fig. 3. The highest conductivity value of  $6.3 \times 10^{-4} \text{ S cm}^{-1}$  at  $25^\circ\text{C}$  was obtained for the composition at  $x = 78.4$ , which is comparable to the  $80\text{Li}_2\text{S} \cdot 20\text{P}_2\text{S}_5$  glass-ceramics with the thio-LISICON II analogue ( $7.2 \times 10^{-4} \text{ S cm}^{-1}$ ) [12] and is higher than the  $\text{Li}_{3+5x}\text{P}_{1-x}\text{S}_4$  system ( $1.5 \times 10^{-4} \text{ S cm}^{-1}$ ) prepared by solid state reaction [8].

Fig. 4 shows the compositional dependence of the room-temperature-conductivities ( $\sigma_{25}$ ) and the activation energies ( $\Delta E_a$ ) determined from Fig. 3. The conductivities are higher than  $10^{-4} \text{ S cm}^{-1}$  over the whole composition range ( $75 \leq x \leq 80$ ), which is believed due to the formation of a highly conductive crystalline phase analogous to the thio-LISICON III phase. The conductivity increases with increasing  $x$  and shows a maximum value of  $6.3 \times 10^{-4} \text{ S cm}^{-1}$  at  $x = 78.3$ .

Kanno and Murayama [7] reported that the thio-LISICON II phase has a special monoclinic superstructure and shows much higher conductivities than the III phases. Although the thio-LISICON III phase was formed in the  $78.3\text{Li}_2\text{S} \cdot 21.7\text{P}_2\text{S}_5$  glass-ceramic, it is noteworthy that the conductivity value of the obtained thio-LISICON III phase is comparable to the  $80\text{Li}_2\text{S} \cdot 20\text{P}_2\text{S}_5$  glass-ceramic with thio-



**Fig. 4.** Composition dependence of the room temperature conductivities ( $\sigma_{25}$ ) and the activation energies ( $\Delta E_a$ ) of the  $x\text{Li}_2\text{S}-(100-x)\text{P}_2\text{S}_5$  glass-ceramics ( $75 \leq x \leq 80$ ) prepared by heat-treatment of mechanically milled powders at  $260^\circ\text{C}$  for 3 h.



**Fig. 5.** Time dependence of DC current after applying a constant DC voltage of 1 V to the  $78.3\text{Li}_2\text{S} \cdot 21.7\text{P}_2\text{S}_5$  glass-ceramic prepared by heat-treatment of mechanically milled powders at  $260^\circ\text{C}$  for 3 h.

LISICON II phase, which is not in agreement with previous report [7].

This controversial result is probably caused by the introduction of interstitial lithium ions at the Li sites which affects the Li ion distribution. It has been reported that the structure of the host material,  $\text{Li}_3\text{PS}_4$  (molar composition of  $75\text{Li}_2\text{S} \cdot 25\text{P}_2\text{S}_5$ ), consists of

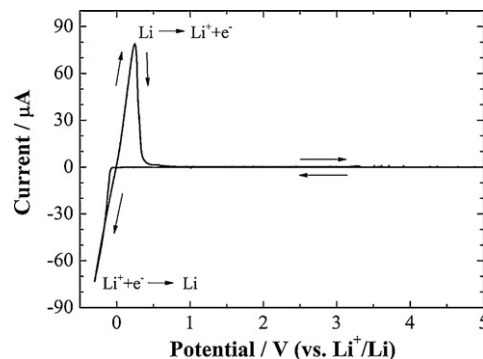


**Fig. 6.** Cyclic voltammogram of the asymmetric  $\text{Li}/78.3\text{Li}_2\text{S} \cdot 21.7\text{P}_2\text{S}_5$  glass-ceramic/SUS cell. The scan rate was  $5 \text{ mV s}^{-1}$ , and the scan ranges were between  $-0.3$  and  $+5.0 \text{ V}$ .

the tetrahedral  $\text{LiS}_4$ ,  $\text{PS}_4$ , and octahedral  $\text{LiS}_6$  units which are connected in three dimensions [8]. Li ion sites which can participate in the ionic conduction are distributed over the tetrahedral Li(2), Li(4) sites and the octahedral Li(5) site. Among these sites, the Li(4) and Li(5) site have partial lithium occupancy. Also, it has been reported that lithium vacancies or interstitial lithium ions were introduced by aliovalent substitutions of  $\text{Si}^{4+} \leftrightarrow \text{Li}^+ + \text{Al}^{3+}$  or  $\text{Si}^{4+} + \text{Li}^+ \leftrightarrow \text{P}^{5+}$  according to the stoichiometric relation of  $\text{Li}_{4+x}\text{Si}_{1-x}\text{Al}_x\text{S}_4$  and  $\text{Li}_{4-x}\text{Si}_{1-x}\text{P}_x\text{S}_4$ , respectively [6].

For  $\text{Li}_2\text{S}-\text{P}_2\text{S}_5$  system, interstitial lithium ions are expected to be introduced in partially occupied interstitial sites (relatively mobile Li(4) and Li(5)) by aliovalent substitution of  $\text{P}^{5+} \leftrightarrow 5\text{Li}^+$ , according to the stoichiometric relation of  $\text{Li}_{3+5x}\text{P}_{1-x}\text{S}_4$ , and this is believed to affect the ionic distribution and the lithium ion mobility.

The decrease of conductivities with increasing  $x$  in the  $x \geq 78.3$  is mainly due to the increase of insulative  $\text{Li}_2\text{S}$  crystals in the samples as supported by XRD data in Fig. 1. The change of activation energies is similar to that of conductivities. The activation energy decreases with  $x$  value in the range of ( $75 \leq x \leq 78.3$ ), and shows a minimum value of  $30.5 \text{ kJ mol}^{-1}$  at  $x = 78.3$ . The position of the minimum in activation energy is the same as that of the maximum in conductivity of the samples indicating that the increase in conductivity is also affected by the decrease in activation energy.

Fig. 5 shows the relaxation of DC current after applying a constant DC voltage of 1 V to the  $78.3\text{Li}_2\text{S}-21.7\text{P}_2\text{S}_5$  glass-ceramic prepared by heat-treatment at  $260^\circ\text{C}$  for 3 h. When the lithium plates were used as non-blocking electrodes, the constant current of  $9.8 \times 10^{-3} \text{ A}$  due to Li ion drift and the leakage current by electrons/holes was observed after 800 s and the conductivity was calculated to  $4.9 \times 10^{-4} \text{ S cm}^{-1}$  at  $20^\circ\text{C}$ , which agreed well with the value obtained from the AC impedance measurement. When the stainless steel plates were used as blocking electrodes, the current exhibited typical space polarization relaxation and then the leakage current of about  $3.5 \times 10^{-9} \text{ A}$  due to electrons/holes was observed after 800 s. The DC conductivity obtained using blocking electrodes is  $1.75 \times 10^{-10} \text{ S cm}^{-1}$  and is about 5 orders of magnitude lower than the one obtained by using the lithium electrodes. Lithium ion transport number of the  $\text{Li}_{3.35}\text{P}_{0.93}\text{S}_4$  sample is calculated to be  $>0.9999$ . These results suggest that the electronic conductivity is almost negligible in the obtained specimen.

Fig. 6 shows the cyclic voltammogram of the asymmetric  $\text{Li}/78.3\text{Li}_2\text{S}-21.7\text{P}_2\text{S}_5$  glass-ceramic/SUS cell. The potential was swept between  $-0.3$  and  $+5.0 \text{ V}$  vs.  $\text{Li}^+/\text{Li}$  and the scan rate was  $5 \text{ mV S}^{-1}$ . A cathodic current peak due to the lithium deposition reaction ( $\text{Li}^+ + \text{e} \rightarrow \text{Li}$ ) is observed on a cathodic sweep from  $-0.3$  to  $0 \text{ V}$ , and then an anodic current peak due to the dissolution reaction of metallic lithium ( $\text{Li} \rightarrow \text{Li}^+ + \text{e}$ ) is observed at around  $+0.2 \text{ V}$  on an anodic sweep. There are no significant current peaks due to the electrolyte decomposition or phase change except the peak corresponding to the deposition and dissolution of lithium over the

whole range from  $-0.3$  to  $+5.0 \text{ V}$ , suggesting the samples have the electrochemical stability under the test conditions.

#### 4. Conclusions

The thio-LISICON structure was synthesized in the mechanically milled amorphous  $\text{Li}_2\text{S}-\text{P}_2\text{S}_5$  system by heat-treatment. The highly conductive crystalline phase analogous to the thio-LISICON III was formed over the whole composition range of  $75 \leq x \leq 80$ , and the  $78.3\text{Li}_2\text{S}-21.7\text{P}_2\text{S}_5$  glass-ceramic shows the highest conductivity of  $6.3 \times 10^{-4} \text{ S cm}^{-1}$  at  $25^\circ\text{C}$ , which is higher than the maximum conductivity reported in the  $\text{Li}_{3+5x}\text{P}_{1-x}\text{S}_4$  system ( $1.5 \times 10^{-4} \text{ S cm}^{-1}$ ) prepared by solid phase reaction and is comparable to the  $80\text{Li}_2\text{S}-20\text{P}_2\text{S}_5$  glass-ceramic with the thio-LISICON II analogue ( $7.2 \times 10^{-4} \text{ S cm}^{-1}$ ). The enhanced conductivities with  $x = 78.3$  are probably caused by the introduction of interstitial lithium ions. The material shows high electrochemical stability and no reaction with lithium metal. The lithium ion transport number of the sample was almost unity, indicating that the electronic conductivity is almost negligible. Therefore, the  $\text{Li}_2\text{S}-\text{P}_2\text{S}_5$  glass-ceramics prepared by mechanical milling and heat-treatment have great potential as high lithium ion conducting solid electrolytes.

#### Acknowledgments

This research was supported by a grant from the Fundamental R&D Program for Core Technology of Materials funded by the Ministry of Knowledge Economy, Republic of Korea.

#### References

- [1] J.M. Tarascon, M. Armand, *Nature* 414 (2001) 359.
- [2] A. Hayashi, S. Hama, F. Mizuno, K. Tadanaga, T. Minami, M. Tatsumisago, *Solid State Ionics* 175 (2004) 683.
- [3] Y. Hashimoto, N. Machida, T. Shigematsu, *Solid State Ionics* 175 (2004) 177.
- [4] P. Knauth, *Solid State Ionics* 180 (2009) 911–916.
- [5] H.Y.-P. Hong, *Mater. Res. Bull.* 13 (1978) 117.
- [6] M. Murayama, R. Kanno, M. Irie, S. Ito, T. Hata, N. Sonoyama, Y. Kawamoto, *J. Solid State Chem.* 168 (2002) 140.
- [7] R. Kanno, M. Murayama, *J. Electrochem. Soc.* 148 (2001) A742.
- [8] M. Murayama, N. Sonoyama, A. Yamada, R. Kanno, *Solid State Ionics* 170 (2004) 173.
- [9] A. Hayashi, Y. Ishikawa, S. Hama, T. Minami, M. Tatsumisago, *Electrochem. Solid State Lett.* 6 (3) (2003) A47–A49.
- [10] K. Iwamoto, N. Aotani, K. Takada, S. Kondo, *Solid State Ionics* 79 (1995) 288–291.
- [11] H. Morimoto, H. Yamashita, M. Tatsumisago, T. Minami, *J. Am. Ceram. Soc.* 82 (1999) 1352.
- [12] A. Hayashi, S. Hama, T. Minami, M. Tatsumisago, *Electrochem. Commun.* 5 (2003) 111.
- [13] T. Ohtomo, F. Mizuno, A. Hayashi, K. Tadanaga, M. Tatsumisago, *Solid State Ionics* 177 (2006) 2753–2757.
- [14] T. Ohtomo, F. Mizuno, A. Hayashi, K. Tadanaga, M. Tatsumisago, *Solid State Ionics* 176 (2005) 2349–2353.
- [15] Z. Zhang, J.H. Kennedy, *Solid State Ionics* 38 (1990) 217.